High-Temperature Crystalline and Molecular Structures of the Main-Chain Thermotropic Polyester Poly[(oxydodecanedioyl)oxy-1,4-phenylene(2-methylvinylene)-1,4-phenylene]. An Application of the Fiber Whole-Pattern Method

Maurizio Carotenuto and Pio Iannelli*

Dipartimento di Fisica, Università di Salerno, I-84100 Salerno, Italy

Received February 6, 1992; Revised Manuscript Received April 24, 1992

ABSTRACT: The molecular structure of the crystalline phase of the thermotropic main-chain polyester known as $C_{12}\alpha$MS, stable at 175 °C, has been determined by fiber X-ray diffraction using the whole-pattern method. The polymer has a complex polymorphism, and the phase characterized is the one stable just below the transition to the nematic state. The unit cell is monoclinic, $P2_1/a$ space group with two repeat unit $C_{14}H_{16}O_2$ per cell. Lattice constants are a = 13.83 (1) Å, b = 5.28 (1) Å, c = 27.3 Å, and β = 138.6°. Due to the strong thermal motion of the carbon and hydrogen atoms of the aliphatic sequence along the molecular chain, the phase has been classified as a disordered crystal of G type.

Introduction

The title compound is a polymorphic and thermotropic linear polyester belonging to a class of polymers termed $C_n\alpha$MS (MS = methylstilbene) with the formula

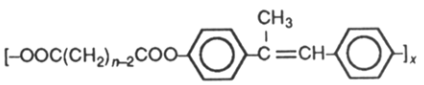

The interest of these polymers is in their mesogenic properties. The $C_{12}\alpha$MS polymer has three crystalline phases (fibrous structures) and a nematic phase. The present study concerns the crystalline phase stable just below the nematic state, and its elucidation has allowed us to understand the nature of the residual order in the nematic state and also to infer the principal features of the lower-temperature crystalline phase.

The X-ray diffraction spectra at room temperature reveals high crystallinity and a high degree of orientation. Because the phase studied by us has however few observable diffraction spots, the structural analysis takes advantage of using the whole-pattern method recently introduced[1–8] for studying fibrous crystalline materials. The method avoids the peak-deconvolution process for evaluating integrated diffraction intensities and is also applicable, by means of "internal coordinates" (bond lengths, bond and torsion angles, etc.), to structures with large unit cells and few observable Bragg reflections in the experimental pattern.

Polymorphism and Diffraction Measurements

$C_{12}\alpha$MS has been synthetized by interfacial polymerization as outlined by Roviello and Sirigu[9–11] who discovered its polymorphic behavior by DSC and diffraction methods. The DSC measurements were repeated by us in a new material, and the DSC trace (see Figure 1) displays the same features already found, which are two sharp crystal–crystal transitions at 135 and 165 °C, a sharp crystalline–nematic transition at 185 °C, and a nematic–isotropic liquid transition at about 210 °C. The crystalline phases have been labelled I, II, and III, respectively.

Fiber diffraction spectra of phase III were recorded at 175 °C using fibrous samples of $C_{12}\alpha$MS obtained by extruding the polymer in the nematic state without any further treatment. Photographic technique and a flat camera have been employed (Figure 2).

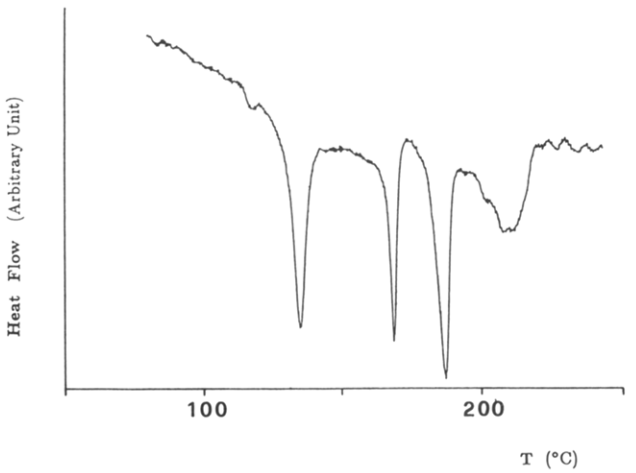

Figure 1. DCS trace of $C_{12}\alpha$MS after annealing 3 h at 175 °C.

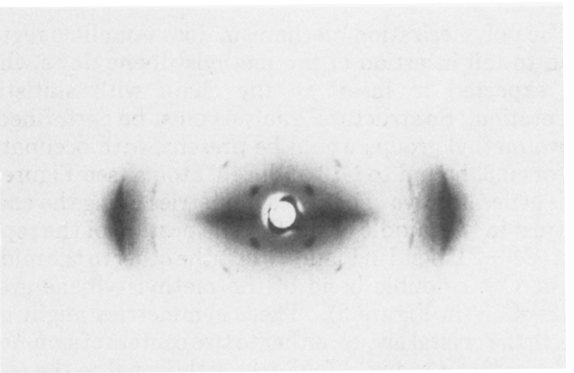

Figure 2. X-ray diffraction pattern (flat camera) from a fiber sample of $C_{12}\alpha$MS phase III at 175 °C.

Temperature was controlled by a homemade heater with an absolute error of about ±3 °C. The vanadium filtered Cr Kα radiation was employed to improve resolution. Two spectra with an exposure ratio of 1:10 have been recorded, to overcome the limited linearity range of photographic emulsion. The two films were then digitized by a photoscan Instrument (Optronics System P1000, Model 30D) using the 100- × 100-μm window and merged in a single 2.0- × 4.5-cm pattern. The preliminary data processing for obtaining diffraction intensity data from the optical density measurements followed the procedure outlined in

0024-9297/92/2225-4373$03.00/0

Table I
Observed and Calculated Reciprocal Coordinates ζ and ξ ($Å^{-1}$) of the Bragg Reflection *hkl* for $C_{12}\alpha$MS Phase III at 175 °C[a]

hkl	ξ_{obsd}	ζ_{obsd}	ξ_{calcd}	ζ_{calcd}
110 + 1$\bar{1}$0 + 200	0.219	0.0	0.219	0.0
001	0.0412	0.0364	0.0412	0.0366
$\bar{2}$01	0.178	0.0365	0.177	0.0366
$\bar{1}$11 + $\overline{1\bar{1}1}$			0.201	0.0366
111 + 1$\bar{1}$1			0.242	0.0366
201	0.261	0.0367	0.260	0.0366
002	0.0833	0.0735	0.0832	0.0734
$\bar{2}$02	0.133	0.734	0.135	0.0734
$\bar{2}$03	0.0945	0.111	0.0943	0.110
003	0.127	0.110	0.124	0.110

[a] The refined cell parameters a = 13.83 Å, b = 5.28 Å, c = 27.3 Å, and β = 138.6° have been employed.

refs 1–5. The background intensity due to incoherent scattering and to the amorphous material was not subtracted ab initio and was considered at the subsequent fitting stage.

Preliminary Analysis of Structure

Structure of $C_{12}\alpha$MS phase III has been investigated on the basis of the X-ray diffraction pattern at 175 °C (see Figures 2 and 4a).

The first step was to find the unit cell, chain symmetry, and crystal symmetry. Indeed, Petraccone et al.[12] proposed a monoclinic cell with lattice constants a = 14.6 (1) Å, b = 5.2 (1) Å, c = 27.5 (6) Å, β = 40 (2)°, and V = 1342 $Å^3$ (c fiber axis). This cell, with small differences in parameters, fits the phase III spectrum with all indexed reflections belonging to the $h + k = 2n$ class (see Table I). As reflections 200 and 110 are both calculated strong (see below) whilst only one sharp spot is detectable in the spectrum, Petraccone's cell was slightly adjusted by imposing the condition $a(\sin\beta)/b = \sqrt{3}$, which ensures the exact overlap of the 110 and 200 reflections (*equatorial pseudohexagonal packing*) and, thus, the lattice constants were adjusted to a = 13.83 Å, b = 5.28 Å, c = 27.3 Å, and β = 138.6°.

The polymerization mechanism does not allow regular head-to-tail insertion of the methylstilbene units which are expected to insert in the chain with statistical orientation. So structural analysis must be performed as if two methyl groups would be present, with occupation factors 0.5, bound to C13 and C13′ atoms (see Figure 3). This generates two *chemical* symmetries along the chain, one just in the middle of the flexible portion of the repeat unit (C1—C1′ bond in Figure 3) and the other in the middle of the C=C double bond of the methylstylbene group (C13=C13′ in Figure 3). These symmetries might give rise, in the crystal lattice, either to two centers of symmetry in the chain or to two 2-fold axes orthogonal to the chain axis. The latter, however, would imply no realistic chain conformations causing strong intramolecular steric interactions. So the only reliable chain symmetry is the inversion centers.

As the repeat unit of the polymer has, in the most extended conformations, about the length of the c axis, the unit cell must contain a single repeat unit along the chain, but due to cell volume, two chains per cell. In the preliminary hypothesis that chain symmetry is the inversion center and that crystal symmetry has an inversion center, the $P2_1/a$ space group seems to be reliable for beginning structure analysis.

As few data are available, whilst the size of crystallographic asymmetric unit is rather large, it is necessary to use a structure analysis approach based on "internal" coordinates rather than atomic ones, keeping constant all predictable quantities. So we fixed most of the internal coordinates for modeling chain conformation according to Table II,which are all the bond lengths l_i, for which all usual standard values were assumed, all the C–C–C bond angles ϕ_i set to 109.5° (sp^3 geometry) or 120° (sp^2 geometry), and the torsion angles τ_i controlling the $-(CH_2)_{10}-$ segment conformation kept fixed to 180°. The latter angles indeed should be close either to 180° or to

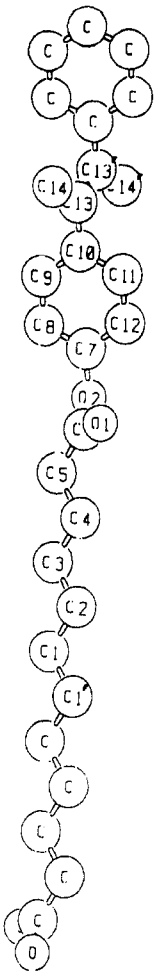

Figure 3. $C_{12}\alpha$MS unit. The atoms are labeled.

Table II
Structural Parameters Defining the Molecular Conformation for $C_{12}\alpha$MS[a]

Distances (Å)			
l_1 C–H	1.08	l_2 C–C	1.54
l_3 C–CO	1.50	l_4 C=O	1.25
l_5 C=C (double bond)	1.33	l_6 C=C (phenyl)	1.40
l_7 O–C	1.40	l_8 OC–O	1.30
Angles (deg)			
τ_1 C1′–C1–C2–C3	180	τ_2 C1–C2–C3–C4	180
τ_3 C2–C3–C4–C5	180	τ_4 C3–C4–C5–C6	180
τ_5 C4–C5–C6–O2		τ_6 C5–C6–O2–C7	
τ_7 C6–O2–C7–C8		τ_8 C9–C10–C13–C13′	
ϕ_1 C1′–C1–C3	109	ϕ_2 C1–C2–C3	109
ϕ_3 C2–C3–C4	109	ϕ_4 C3–C4–C5	109
ϕ_5 C4–C5–C6	109	ϕ_6 C5–C6–O2	120
ϕ_7 C6–O2–C7	120	ϕ_8 O2–C7–C8	120
ϕ_9 C7–C8–C9	120	ϕ_{10} C9–C10–O13	120
ϕ_{11} C10–C13–C13′	120	ϕ_{12} C5–O6–O1	120
ϕ_{13} C10–C13–C14	120		

[a] Only the values for those structural parameters kept fixed during the refinement are given.

±60° to give staggered conformation, but any combination with $\tau_i \neq 180°$ gives rise to a chain repeat shorter than 27.3 Å (chain repeat resulting from c axis). As it is necessary to reduce at most the number of variables, we fixed the above τ_i angles to the 180° value. So the chain conformation depends on six parameters only: ϕ_6 and ϕ_7 bond angles and τ_5, τ_6, τ_7, and τ_8 torsion angles, as defined in Table II.

To complete the crystal structure model, the overall translations and overall rotation Φ_0 must be also defined. The former however is a matter of origin fixing. Following the $P2_1/a$ hypothesis, we put the inversion center halfway between C1 and C1′ atoms at the cell origin. The overall rotation of the chain is constrained by the crystal packing owing to the methyl group, and only with it lying quite parallel to the 010 plane, do reliable atom-to-atom contacts take place. In order to reduce the unknowns, the methyl group has been placed exactly parallel to the 010 plane ($\Phi_0 = 0$) in the preliminary stage.

Initially, the structural model has been adjusted by trial. The four torsion angles τ_5, τ_6, τ_7, and τ_8 and the bond angles ϕ_6 and ϕ_7 were evaluated both by considering that the repeat must match the c edge (fiber axis) and the coarse values of diffracted intensities. We obtained $\tau_5 = 220°$, $\tau_6 = 200°$, $\tau_7 = 60°$, $\tau_8 = 90°$, $\phi_6 = 120°$, and $\phi_7 = 120°$. These values were used as the starting point for the subsequent refinement stage.

Structure Refinement Using the Fiber Whole-Pattern Method

A short description of the whole-pattern method applied to fibrous structure seems opportune. The method[1-6] consists of fitting the X-ray fiber diffraction pattern with the one calculated as a function of structural parameters. Using the least squares procedure, one obtains the "best parameters" minimizing the quantity

$$\sum_i w_i [I_{obsd}(\rho_i,\sigma_i) - S_j I_{calcd}(\rho_i,\sigma_i)]^2 \quad (1)$$

where w_i are the statistical weights of the observations $I_{obsd}(\rho_i,\sigma_i)$, ρ_i is the scattering vector $2(\sin\theta_i)/\lambda$, and σ_i is the angle between ρ_i and the fiber axis. As many scale factors S_j are considered as the number n of films measured. According to refs 5 and 6, the calculated diffraction intensity $I_{calcd}(\rho_i,\sigma_i)$ in the reciprocal space is obtained by

$$I_{calcd}(\rho_i,\sigma_i) = S\sum_k I_k{}^2 T_k(\rho_i - \rho_k, \sigma_i - \sigma_k) + B(\rho_i,\sigma_i) \quad (2)$$

The sum is extended over all reflections whose Bragg ρ_k, σ_k points are close to the current ρ_i, σ_i one. I_k is the *integrated intensity* which depends on the molecular structure and is defined as $I_k = mPF_k^2$ where m is the multiplicity, P is the polarization factor, and F_k is the structural factor. S is a scale factor, T_k is the profile function for the kth Bragg reflection, and $B(\rho_i,\sigma_i)$ is the diffused diffraction intensity due to amorphous material and air. In the present case the last term has been parametrized considering[5] (i) the contribution of uncoherent scattering depending on the ξ_i and ζ_i components of ρ_i and (ii) a contribution of diffraction of noncrystalline but oriented material appearing in the spectra as a weak streak along the equatorial line. Thus $B(\rho_i,\sigma_i)$ is

$$B(\rho_i,\sigma_i) = B(\xi_i,\zeta_i) = B^u(\xi_i,\zeta_i) + B^a(\xi_i,\zeta_i) \quad (3)$$

$$B^u(\xi_i,\zeta_i) = \epsilon_1 + \epsilon_2\xi_i + \epsilon_3\xi_i^2 + \epsilon_4\zeta_i + \epsilon_5\zeta_i^2 \quad (3.1)$$

$$B^a(\xi_i,\zeta_i) = \frac{f_1}{f_2 f_3}\exp\left[-\left(\frac{\xi_1 - f_4}{f_2}\right)^2\right]\exp\left[-\left(\frac{\zeta_i}{f_3}\right)^2\right] \quad (3.2)$$

According to ref 5, the T_k profile function depends on the crystallite sizes Δa, Δb, and Δc, taken respectively along the cell axes a, b, and c, and the misalignment parameter α_0, which is the *full width at half-maximum* (*fwhm*) of the Gaussian alignment distribution function of crystallites around the fiber axis.

All the parameters ϵ_i and f_i in eqs 3 are nonstructural ones, and they do not affect the integrated intensity I_k in eq 2, which depends only on the structural parameters. The optimization of both structural and nonstructural parameters is performed by a least squares procedure. As usual, the latter is based on the Gauss–Newton linearization of the observational equations and the process must be iterated till low shift to standard error ratios are obtained.

In our case the strategy adopted to refine the structure of $C_{12}\alpha$MS was the following: (1) In all the refinements the chain continuity was accounted for by using the Lagrange multiplier according to refs 3 and 13. (2) Firstly, we refined the nonstructural parameters defining the background B and the profile function T_k. Having fixed $S_1 = 1$, we have $S_2 = 10$ according to the exposure time ratio. The cell parameters were taken fixed to the values $a = 13.83$ Å, $b = 5.29$ Å, $c = 27.3$ Å, and $\beta = 138.6°$. The structural parameters were fixed to the values given in Table II and to those obtained in the preliminary "trial and error" stage. The *film-to-sample* distance was evaluated to be 59.7 mm by a powder sample of NaCl as standard, and it was kept constant during the refinement. (3) The structural parameters τ_5, τ_6, τ_7, τ_8, and Φ_0 were refined altogether with the nonstructural ones, except the scale factor S_2. The isotropic thermal B_{iso} parameter, equal for all atoms, was fixed to 2.0 Å^2, and it was kept constant. (4) All the parameters were refined altogether, including scale factor S_2 and lattice constants a and b with the constrained condition $b = a(\sin\beta)/\sqrt{3}$. Trials to include β and c in the refinement failed (very few visible reflections).

The observed–calculated agreement (see Figure 4) is good, except for the 111 reflection, which is undetectable in the experimental pattern but quite visible in the calculated one, and the 001 reflection, which is calculated weaker than the experimental one.

To improve the fitting, we considered in the structural model a strong thermal atomic motion. As a consequence of the molecular packing (see later), the aliphatic portion of adjacent chains are close with respect to each other (see Figure 5a). In the adopted hypothesis of all-trans conformation, two carbon atoms in sequence along the chain filled up a volume of about 60.6 Å^3, which corresponds to a local density of 0.77 g/cm^3. It is worth noting that the liquid density of polyethylene extrapolated to 175 °C is about 0.77 g/cm^3,[14] suggesting that the aliphatic sequence in the chain is thermally disordered. On the other hand the methylstilbene rigid sequence is tightly packed. The effect of such a disorder on the diffraction pattern maybe accounted for if one keeps in mind that the aliphatic sequence is still in the most extended conformation, as deduced from the axis length, and that disorder should take place only perpendicular to the chain. This suggests the use of an anisotropic thermal ellipsoid for describing

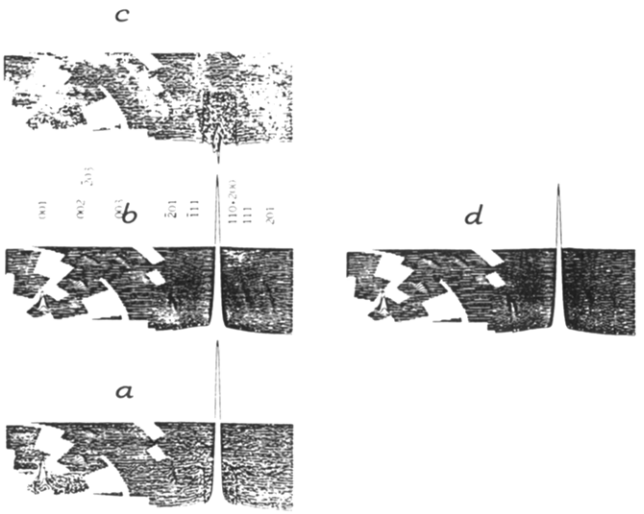

Figure 4. Comparison between the observed (a) and the calculated (b) diffraction pattern, with the relative difference (c), for a fiber sample of $C_{12}\alpha$MS phase III at 175 °C. Isotropic thermal factors have been employed. The calculated pattern obtained by using anisotropic thermal factors is also shown (d).

the atomic motion with one axis of the ellipsoid perpendicular to the chain axis. Consequently, the thermal factor f_t should be defined as

$$f_t = \exp\left[-\frac{1}{4}(B_\parallel \rho_\parallel^2 + B_\perp \rho_\perp^2)\right] \quad (4)$$

where $\rho_\parallel$ and $\rho_\perp$ are respectively the parallel and perpendicular component of the scattering vector with respect to the chain axis.

Thus, starting from the refined parameters' values, we imposed an averaged atomic displacement $\langle u \rangle_\perp = 0.50$ Å only to the carbon and hydrogen atoms of the aliphatic sequence, which corresponds to $B_\perp = 8\pi^2 \langle u \rangle_\perp^2 = 19.7$ Å^2, and we carried out a refinement in order to get only the best value for the scale factor S. Improvement in the fitting is obtained with a weaker 111 and a stronger 001 reflection (see Figure 4d).

The refined parameters are listed in Table III, and a list of fractional atomic coordinates is given in Table IV. The molecular packing is shown in Figure 5.

The intra- and intermolecular atomic distances are in agreement with the standard values, except the intramolecular distance between the carbonyl oxygen atom and the methyl carbon atom which is only 2.88 Å. A higher degree of freedom might avoid such a steric interaction because the torsion angles along the aliphatic sequences, which have been kept fixed during refinement to reduce the number of parameters, strongly affect the carbonyl group position.

Conclusions

The molecular structure of $C_{12}\alpha$MS phase III, including thermal disorder, accounts for the X-ray experimental diffraction pattern at 175 °C. The whole-pattern method has been applied successfuly, showing that it is a good tool for carrying out molecular structure refinement even if few diffraction spots are observed in the pattern.

In our opinion the torsion angles which have been fixed may really fluctuate, provided that chain length is reproduced. As a consequence, the molecular structure we report should be regarded as a representation of a *dynamic structure*.

The molecular packing is that observed both in the smectic S_F phase and disordered crystalline G phase. Since there is no loss of *long-range order* but only the presence

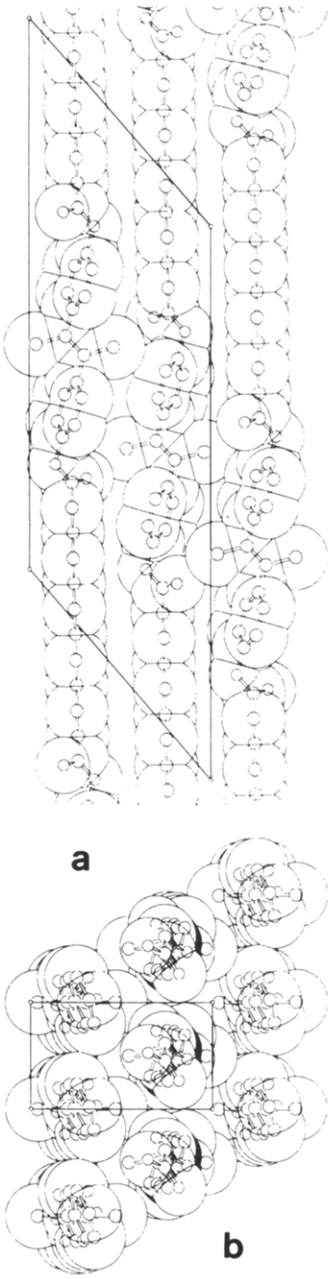

Figure 5. Molecular packing for $C_{12}\alpha$MS phase III: (a) view along the b and (b) along the c axis.

Table III
Structural and Nonstructural Parameters As Obtained after Refining the Structure

$\tau_5 = 223.4$ (2)°	$\tau_6 = 219.7$ (2)°	$\tau_7 = 88.1$ (6)°	$\tau_8 = 111.6$ (6)°
$\Phi_0 = 0.0$ (6)°			
$\Delta a = 1450$ (20) Å	$\Delta b = 150$ (5) Å	$\Delta c = 298$ (5) Å	$\alpha_o = 6.67$ (3)°
$a = 13.83$ (1) Å	$b = 5.29$ (1) Å	$c = 27.3$ Å	$\beta = 138.6$°
$S = 8.99$ (3)	$S_2 = 9.55$ (2)		
$\epsilon_1 = 12.45$ (2)	$\epsilon_2 = -22.7$ (2)	$\epsilon_3 = 14.7$ (7)	$\epsilon_4 = -13.0$ (4)
$\epsilon_5 = -205$ (3)			
$f_1 = 0.0282$ (1)	$f_2 = 0.0320$ (1)	$f_3 = 0.0901$ (1)	$f_4 = 0.2120$ (2)

of a strong thermal disorder, the phase should be classified as a disordered crystal of G type.[15] The molecules are packed building parallel *sheets* which are shifted with respect to each other by $|a(\cos\beta)/2| = 5.18$ Å along the c axis direction. The transition to the nematic phase at about 210 °C could be explained with the loss of correlation between neighbor molecules which become free to shift along the c axis. This causes the disappearance of all the meridional reflections.

Table IV
Fractional Atomic Coordinates for $C_{12}\alpha$MS Phase III at 175 °C

atom	*x*	*y*	*z*
O1	0.065 (3)	0.232 (3)	0.284 (7)
O2	−0.109 (3)	−0.0236 (5)	0.243 (9)
C1	−0.004 (1)	−0.088 (1)	0.021 (1)
C2	−0.003 (1)	0.075 (1)	0.068 (1)
C3	−0.011 (2)	−0.100 (1)	0.110 (1)
C4	−0.009 (1)	0.063 (2)	0.157 (3)
C5	−0.018 (1)	−0.113 (2)	0.200 (3)
C6	−0.016 (2)	0.046 (2)	0.245 (4)
C7	−0.069 (2)	−0.018 (2)	0.308 (3)
C8	−0.001 (1)	−0.228 (2)	0.355 (3)
C9	0.039 (2)	−0.223 (3)	0.420 (2)
C10	0.011 (1)	−0.007 (1)	0.438 (3)
C11	−0.057 (2)	0.203 (2)	0.390 (2)
C12	−0.097 (2)	0.197 (2)	0.326 (3)
C13	0.051 (1)	−0.001 (1)	0.502 (3)
C14	0.214 (2)	0.003 (1)	0.578 (3)

The polymorphism of $C_{12}\alpha$MS can be partially explained on the basis of the molecular structure of phase III: phase I at 120 °C shows a diffraction pattern similar to that from phase III at 175 °C, but with quite strong $\bar{1}11 + \bar{1}\bar{1}1$ and $111 + 1\bar{1}1$ peaks. Further analysis to solve the molecular structure of phases II and I is still in progress.

Acknowledgment. We are grateful to Prof. Immirzi, University of Salerno, and Profs. Roviello and Sirigu, University of Naples, for helpful discussion. Financial support by CNR is also acknowledged.

References and Notes

(1) Immirzi, A.; Iannelli, P. *Macromolecules* **1988**, *21*, 768.
(2) Iannelli, P.; Immirzi, A. *Macromolecules* **1989**, *22*, 196.
(3) Iannelli, P.; Immirzi, A. *Macromolecules* **1989**, *22*, 200.
(4) Iannelli, P.; Immirzi, A. *Macromolecules* **1990**, *23*, 2375.
(5) Iannelli, P.; Immirzi, A. XVth Congress of IUCr, Bordeaux, 1990; *Acta Crystallogr.* **1990**, *A46*, C-54.
(6) Iannelli, P. Manuscript in preparation.
(7) Busing, W. R. *Macromolecules* **1990**, *23*, 4608.
(8) Busing, W. R. Regional Meeting of the American Chemical Society, Toledo, OH, July 1991.
(9) Roviello, A.; Sirigu, A. *Makromol. Chem.* **1980**, *181*, 1799.
(10) Roviello, A.; Sirigu, A. *Makromol. Chem.* **1982**, *183*, 895.
(11) Roviello, A.; Sirigu, A. *Makromol. Chem.* **1982**, *183*, 409.
(12) Petraccone, V.; Roviello, A.; Sirigu, A.; Tuzi, A.; Martuscelli, E.; Pracella, M. *Eur. Polym. J.* **1990**, *16*, 261.
(13) Tadokoro, H. *Structure of Crystalline Polymers*; J. Wiley & Sons: New York, 1979; pp 136–144 (see also references therein).
(14) Hunter, E.; Oakes, W. G. *Trans. Faraday Soc.* **1945**, *41*, 49.
(15) Leadbetter, A. J. In *Thermotropic Liquid Crystals*; Gray, G. W., Ed.; J. Wiley & Sons: New York, 1987; Chapter 1 (see also references therein).

Registry No. $C_{12}\alpha$MS (copolymer), 74108-71-7.